Supramolecular Chemistry

DOI: 10.1002/ange.200900063

A Supramolecular Approach for Preparation of Size-Controlled Nanoparticles**

Hao Wang, Shutao Wang, Helen Su, Kuan-Ju Chen, Amanda Lee Armijo, Wei-Yu Lin, Yanju Wang, Jing Sun, Ken-ichiro Kamei, Johannes Czernin, Caius G. Radu,* and Hsian-Rong Tseng**

Over the past decades, significant efforts have been devoted to explore the use of nanoparticles in the fields of biology and medicine. Several different types of nanoparticles have successfully made their way into preclinical studies in animals, clinic trials in patients, or even successful commercial products used in routine clinical practice.[1] For example, gold nanoshells,[2] quantum dots,[3,4] and super-paramagnetic nanoparticles[5] that carry target-specific ligands have been employed for in vivo imaging of cancerous cells; drug molecules have been packaged into polymer-based nanoparticles and/or liposomes[6,7] to achieve controlled release at the disease sites;[8,9] and positively charged nanoparticles have served as nonviral delivery systems for both in vitro and in vivo genetic manipulation and programming.[1,10,11] However, there remains an imperious desire to develop novel synthetic approaches to produce a new generation of nanoparticles that have 1) controllable sizes and morphologies, 2) low toxicity, compatible immunogenicity and in vivo degradability, and 3) proper surface charges and chemistry for improved physiological stability and longer circulation time. Moreover, multiple functions,[12] such as reporter systems for real-time monitoring with imaging techniques (i.e., optical imaging, magnetic resonance imaging (MRI), and positron emission tomography (PET)), targeting ligands for disease-specific delivery, and a controllable mechanism for packaging and releasing drugs and genes, will be conferred to individual nanoparticles for conducting multiple applications in parallel.

Unlike conventional chemical synthesis, which is capable of forming/breaking covalent bonds, supramolecular chemistry combines two basic concepts: self assembly and molecular recognition. Supramolecular chemistry offers a powerful and convenient approach for the preparation of nanostructured materials from molecular building blocks.[13–18] The concept of self-assembly has been extensively used to prepare organic nanoparticles. For example, liposomes and nanoscaled vesicles[7] which were prepared using self-assembly of phospholipids can serve as powerful nanocarriers for drug and gene delivery; self-assembled amphiphilic copolymer building blocks spontaneously form nanoparticles, which can be utilized for drug delivery and molecular imaging.[19–22] However, it is apparent that the concept of "molecular recognition" seems to be an underappreciated factor, which could lead to much more sophisticated synthetic approaches,[23] allowing precise control over the properties of the resulting nanoparticles. β-Cyclodextrin (CD) is one of the most commonly used supramolecular building blocks for a diverse range of biomedical applications.[24,25] CD-containing cationic polymers have been employed as vectors for highly efficient delivery of siRNA. Through CD/adamantane (Ad) recognition, Ad-functionalized polyethylene glycol (PEG) chains were grafted onto the nanoparticles to enable long-term systemic circulation in vivo.[26]

Herein, we report a convenient, flexible, and modular synthetic approach (Figure 1) for the preparation of size-controllable supramolecular nanoparticles (SNPs). CD/Ad recognition was employed to achieve self-assembly of SNPs from three different molecular building blocks, namely 1) Ad-grafted first-generation polyamidoamine dendrimer, *n*-Ad-PAMAM, 2) β-CD-grafted branched polyethylenimine (MW = 10 kD), CD-PEI, and 3) Ad-functionalized PEG compound (MW = 5 kD), Ad-PEG. Although similar to a previously reported "bricks and mortar" strategy[23] to construct cross-linked network,[27] the uniqueness of our design is the use of a capping/solvation group. This solvation group Ad-PEG on the one hand competes with the dendrimer block *n*-Ad-PAMAM to constrain the continuous propagation of the cross-linked network, and on the other hand confers water-solubility to the SNPs. By tuning mixing ratios among the three molecular building blocks in phosphate-buffered saline (PBS) aqueous buffer solution (pH 7.2, containing 1.5 mM KH_2PO_4, 155 mM NaCl, and 2.7 mM Na_2HPO_4), the equilibrium between the propagation/aggregation and capping/solvation of the cross-linked network fragments can be altered, allowing arbitrary control over the sizes of the water-soluble SNPs. In contrast to the production of polymer-based nanoparticles,[19,20,22] where significant synthetic endeavors are required to prepare specific types of polymeric building blocks to achieve the desired level of control over the

[*] Dr. H. Wang,[+] Dr. S. T. Wang,[+] Dr. H. Su,[+] K.-J. Chen, A. L. Armijo, Dr. W.-Y. Lin, Dr. Y. Wang, Dr. J. Sun, Dr. K. Kamei, Prof. J. Czernin, Prof. C. G. Radu, Prof. H.-R. Tseng
Crump Institute for Molecular Imaging (CIMI)
Institute for Molecular Medicine (IMED)
Department of Molecular and Medical Pharmacology
California NanoSystems Institute (CNSI)
University of California, Los Angeles
570 Westwood Plaza, Los Angeles, CA 90095 (USA)
Fax: (+1) 310-206-8975
E-mail: hrtseng@mednet.ucla.edu

[+] These authors contributed equally to the work.

[**] H. R.T. and C.G.R. acknowledge support from the NIH-NCI NanoSystems Biology Cancer Center (U54A119347).

Supporting information for this article is available on the WWW under http://dx.doi.org/10.1002/anie.200900063.

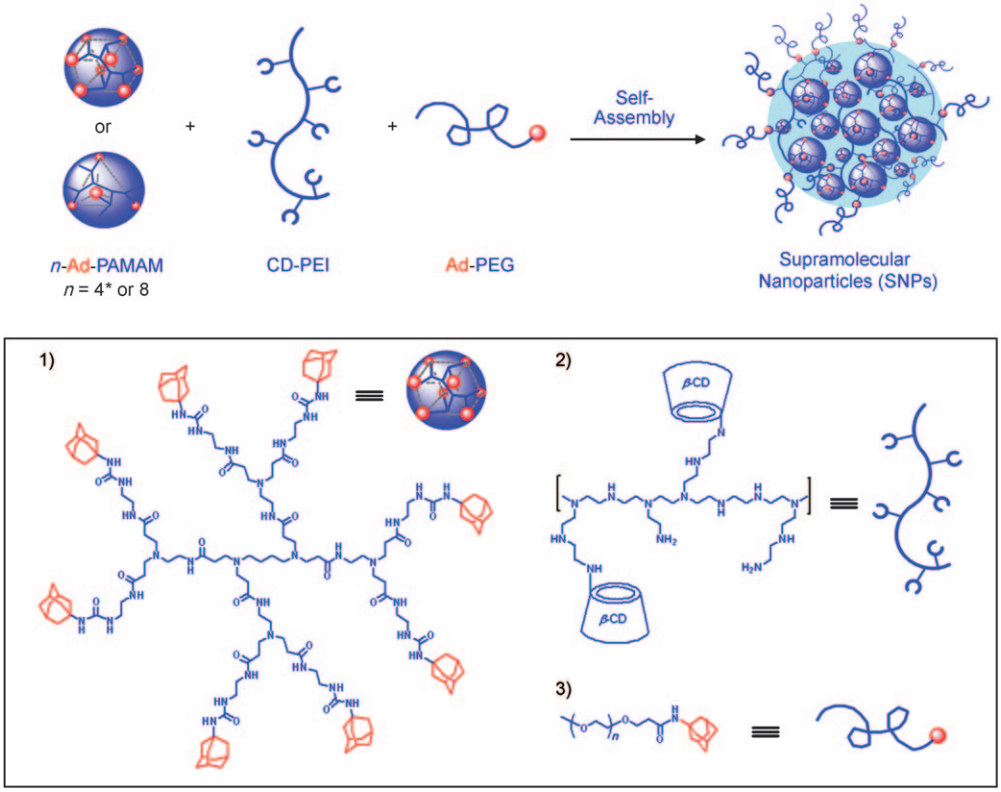

Figure 1. A convenient, flexible, and modular synthetic approach for preparation of size-controlled supramolecular nanoparticles (SNPs). A molecular recognition system based on adamantane (Ad) and β-cyclodextrin (CD) was employed to assemble three molecular building blocks 1) *n*-Ad-PAMAM (*n* = 4* or 8), 2) CD-PEI, and 3) Ad-PEG.

size, our three-component supramolecular approach offers synthetic convenience, flexibility, and modularity to alter the sizes and surface chemistry of the SNPs. By using such a supramolecular approach we were able to obtain a collection of SNPs with controllable sizes ranging from 30 to 450 nm. Further studies were carried out to unveil the unique properties of these SNPs, including 1) their stability at different temperatures and pH values, as well as in physiological ionic strength media, 2) their competitive disassembly in the presence of Ad molecules, and 3) reversible control over the size using in situ alteration of the mixing ratios of the molecular building blocks. Finally, whole-body biodistribution and lymph node drainage studies of both of the 30 and 100 nm ^{64}Cu-labeled SNPs in mice were carried out using microPET/CT imaging. The results showed that the sizes of SNPs are crucial factors which affect their in vivo properties.

The three molecular building blocks *n*-Ad-PAMAM, CD-PEI, and Ad-PEG were prepared and characterized (Supporting Information, Section 1.2). According to the ^{1}H NMR spectrum, in the polymer building block CD-PEI, there are about 7 to 8 CD recognition units grafted on a branched PEI backbone. It is well known that the CD modification increases the biocompatibility and reduces the toxicity of the PEI compounds.[28] In our experiments, two different dendrimer building blocks, 8-Ad-PAMAM with eight substituted Ad motifs and 4*-Ad-PAMAM[29] with four Ad motifs (on average, based on its ^{1}H NMR spectrum), were examined in parallel. To analyze how the mixing ratios between Ad-PAMAM and CD-PEI affect the sizes of the resulting SNPs, we utilized dynamic light scattering (DLS, N4 plus, USA) measurements to analyze the freshly prepared SNPs. To ensure sufficient supply of the capping/solvation group, an excess amount of Ad-PEG was added to each mixture. In the absence of Ad-PEG, direct mixing of *n*-Ad-PAMAM and CD-PEI resulted in aggregation and precipitation. The octa-substituted dendrimer 8-Ad-PAMAM was first tested. In this case, CD-PEI (168 μM) in PBS buffer was slowly added into the mixtures containing Ad-PEG (840 μM) and a variable amount (84 to 672 μM) of 8-Ad-PAMAM. A collection of water-soluble SNPs with variable sizes ranging between 30 and 450 nm were obtained (Figure 2a). The surface-charge densities of SNPs (with diameters ranging from 30 to 450 nm) were determined by zeta potential (ζ) measurements in PBS buffer solution (Zetasizer Nano, Malvern Instruments Ltd), which suggest that the SNPs carry zeta potentials in the range of (16.8 ± 1.2) to (28.5 ± 1.1) mV (Supporting Information, Figure S1). To ascertain the influence of the number of the Ad-substitution groups in a dendrimer core on the sizes of the respective SNPs, the tetra-substituted dendrimer 4*-Ad-PAMAM was also examined. SNPs with relative smaller sizes (30–120 nm) were obtained under similar self-assembly conditions. The morphology and size of the SNPs were also examined by using transmission electron microscopy (TEM, Philips CM-120). The TEM images suggest that the SNPs

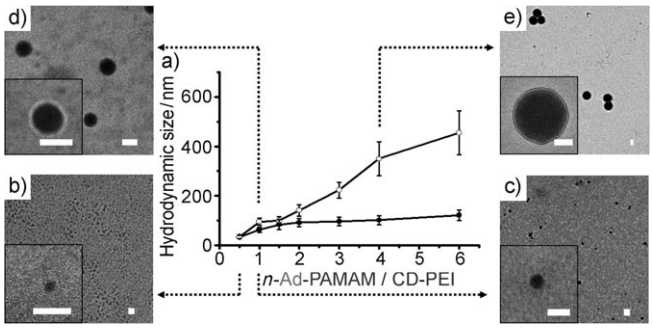

Figure 2. a) Titration plots summarize the relationship between SNP sizes and the mixing ratios of the two molecular building blocks (*n*-Ad-PAMAM/CD-PEI). Dynamic light scattering (DLS) was employed to measure SNP sizes. The titration plot for an octa-substituted dendrimer building block 8-Ad-PAMAM (○) and for a tetra-substituted dendrimer building block 4*-Ad-PAMAM (●). The standard deviation of each data point was contained from, at least, three repeats. TEM images of the resulting SNPs with different sizes of b) (32 ± 7) nm from 8-Ad-PAMAM, c) (61 ± 17) nm from 4*-Ad-PAMAM, d) (104 ± 16) nm from 8-Ad-PAMAM, and e) (340 ± 46) nm from 8-Ad-PAMAM. Scale bars: 100 nm.

exhibit spherical shapes and narrow size distributions (Figure 2b–e; Supporting Information, Figure S2), findings that are consistent with those observed using DLS.

The use of the supramolecular approach conferred dynamic characteristics to the self-assembled SNPs. To understand the dynamic stability of the SNPs, we employed real-time DLS measurements to monitor the size variation of the 30 and 100 nm SNPs (composed of the 8-Ad-PAMAM-based dendrimer) at different temperatures and pH values, and in physiological ionic strength media. First, the variable-temperature DLS measurements indicate that the SNPs are stable over a wide range of temperatures (7 to 50 °C; Supporting Information, Figure S4). Second, we observed negligible size variation of the SNPs at different pH values (pH 3.8–8.3) and physiological ionic strength (Supporting Information, see Figure S3 and S5). We note that the stability of these SNPs can be attributed to the multivalent CD/Ad recognition, which holds individual molecular building blocks in each SNP. Two sets of experiments were carried out to examine the dynamic characteristics (i.e. control of competitive disassembly and reversible alteration of the size) of these SNPs, which further validate the molecular mechanism of this supramolecular approach (Figure 3). First, we introduced 100 equivalents of a competitive reagent (i.e., 1-adamantamine hydrochloride) into a solution containing either 30 or 100 nm SNPs. After 10 minutes of sonication, disassembly of the SNPs was observed by DLS as a result of competitive inclusion of the free 1-adamantamine hydrochloride into CD-PEI. As a control, without the addition of 1-adamantamine hydrochloride, sonication alone could not disassemble the SNPs (Supporting Information, Figure S6). Second, starting from 100 nm SNPs (8-Ad-PAMAM/CD-PEI = 1:1, mol/mol), we were able to reduce the size of the SNPs to 30 nm by adding the polymer component CD-PEI in situ (8-Ad-PAMAM/CD-PEI = 1:2, mol/mol), or increase the size of the SNPs to 140 nm by adding the dendrimer component 8-Ad-PAMAM in situ (8-Ad-PAMAM/CD-PEI = 2:1, mol/mol). In these studies, 10 minutes of sonication was employed to facilitate the conversion among the three sizes of the SNPs (Figure 3).

We characterized the in vivo biodistribution (Figure 4a; Supporting Information, Figure S7) of the 30 and 100 nm ^{64}Cu-labeled SNPs (composed of the 8-Ad-PAMAM-based dendrimer, see Supporting Information for the SNP-labeling protocols) by systemically injecting the SNPs into mice through the tail veins (Supporting Information, Figure S8d). MicroPET/CT studies suggested that the biodistribution patterns of the 30 and 100 nm SNPs were quite similar (Supporting Information, Figure S8a and b). In both cases, rapid blood clearance through liver accumulation (30–50% ID/g of the SNPs accumulated in the liver within 5 min after injection) was observed, and there was less accumulation in the kidneys (16–20% ID/g) and lungs (8–12% ID/g). A nonlinear two-phase decay fit of the SNPs plasma concentrations yielded initial elimination half-lives of 0.87 and 1.1 minutes for the 30 and 100 nm SNPs, respectively. The terminal elimination half-lives were also quite different (68 minutes for 30 nm SNPs was, and 108 minutes for 100 nm SNPs). Together, the results indicated that the in vivo clearance of the 30 nm SNPs is faster than that of the 100 nm SNPs.

To explore the use of the SNPs for immune modulation, we investigated the lymph node trafficking of both 30 and 100 nm ^{64}Cu-labeled SNPs by using front footpad injection (Supporting Information, Figure S8d). The path of lymph drainage from footpad injections is well known, and hence this is a common method for the delivery of immunological agents.[30] We injected the 30 and the 100 nm SNPs into different sides of the footpads of a mouse, and microPET/CT imaging was carried out for 40 minutes immediately after injection (Figure 4b, left) and 20 hours after injection (Figure 4b, right). We observed that the 30 nm SNPs drained

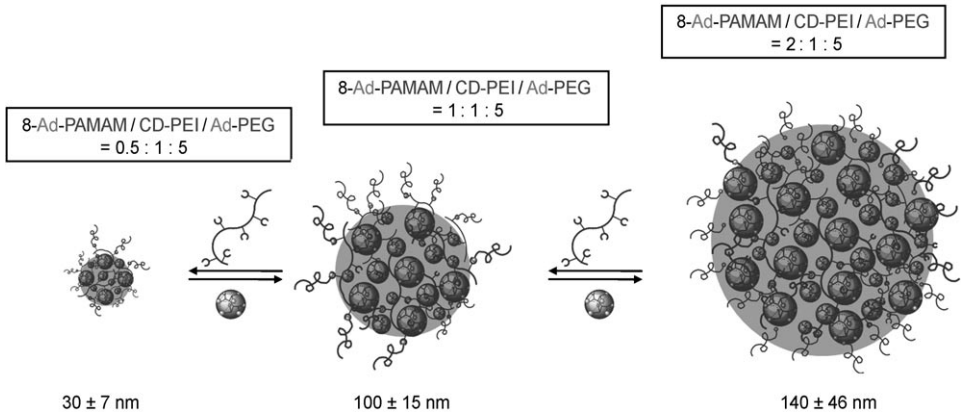

Figure 3. Reversible control of the size of SNPs.

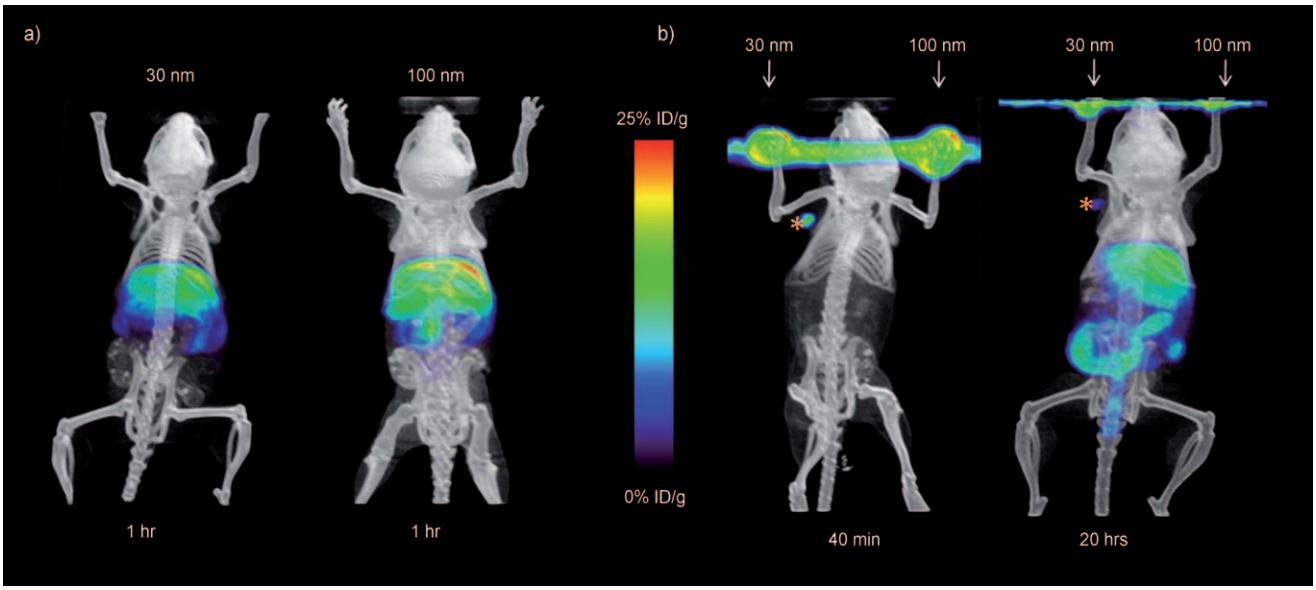

Figure 4. MicroPET/CT studies at various times after injecting the mice with 30 and 100 nm ^{64}Cu-labeled SNPs. a) In vivo biodistribution studies of the SNPs by systemically injecting the SNPs into mice through the tail veins. Left panel: 30 nm SNPs; right panel: 100 nm SNPs. b) Lymph node trafficking studies of SNPs using front footpad injections. The 30 and 100 nm SNPs were injected on different sides of footpads of a mouse. MicroPET/CT was carried out for 40 min immediately after injection (left) and 20 h after injection (right).

into the local auxiliary lymph node and peaked at 5 minutes post injection with (58.6 ± 15.6) % ID/g of signal accumulation (Supporting Information, Figure S8c). This signal decreased to (26.6 ± 5.8) % ID/g at 40 minutes post injection, and further reduced to (7.0 ± 2.2) % ID/g by 20 hours post injection. No significant accumulation was detected in the lymph nodes on the same side where the 100 nm SNPs were injected. Other than the footpad injection site and the lymph node into which the 30 nm SNPs drained, the SNPs did not distribute in vivo to other regions 1 hour after injection. The results revealed that the sizes of the SNPs are critical factors for their lymph node trafficking.

In conclusion, we have successfully developed a convenient, flexible, and modular synthetic approach for the preparation of size-controllable SNPs. PET imaging studies were carried out by injecting ^{64}Cu-labeled SNPs of different sizes into mice. Both whole-body biodistribution and lymph node drainage studies showed that the sizes of the SNPs affect their in vivo characteristics. Besides the imaging studies shown herein, we are currently exploring the use of the size-controllable SNPs for other biomedical applications. Extensive and in-depth study will show the potentials of these SNPs.

Received: January 6, 2009
Published online: May 7, 2009

Keywords: adamantanes · biodistribution · cyclodextrins · nanoparticles · positron emission tomography

[1] M. E. Davis, Z. G. Chen, D. M. Shin, *Nat. Rev. Drug Discovery* **2008**, *7*, 771.
[2] C. Loo, A. Lin, L. Hirsch, M. H. Lee, J. Barton, N. Halas, J. West, R. Drezek, *Technol. Cancer Res. Treat.* **2004**, *3*, 33.
[3] X. Gao, Y. Cui, R. M. Levenson, L. W. Chung, S. Nie, *Nat. Biotechnol.* **2004**, *22*, 969.
[4] S. M. Nie, Y. Xing, G. J. Kim, J. W. Simons, *Annu. Rev. Biomed. Eng.* **2007**, *9*, 257.
[5] Y. W. Jun, J. H. Lee, J. Cheon, *Angew. Chem.* **2008**, *120*, 5200; *Angew. Chem. Int. Ed.* **2008**, *47*, 5122.
[6] J. R. Heath, M. E. Davis, *Annu. Rev. Med.* **2008**, *59*, 251.
[7] V. P. Torchilin, *Nat. Rev. Drug Discovery* **2005**, *4*, 145.
[8] M. E. Napier, J. M. Desimone, *Polym. Rev.* **2007**, *47*, 321.
[9] S. E. Gratton, S. S. Williams, M. E. Napier, P. D. Pohlhaus, Z. Zhou, K. B. Wiles, B. W. Maynor, C. Shen, T. Olafsen, E. T. Samulski, J. M. Desimone, *Acc. Chem. Res.* **2008**, *41*, 1685.
[10] J. J. Green, R. Langer, D. G. Anderson, *Acc. Chem. Res.* **2008**, *41*, 749.
[11] D. W. Pack, A. S. Hoffman, S. Pun, P. S. Stayton, *Nat. Rev. Drug Discovery* **2005**, *4*, 581.
[12] W. B. Cai, X. Y. Chen, *Small* **2007**, *3*, 1840.
[13] C. D. Meyer, C. S. Joiner, J. F. Stoddart, *Chem. Soc. Rev.* **2007**, *36*, 1705.
[14] I. Hwang, W. S. Jeon, H. J. Kim, D. Kim, H. Kim, N. Selvapalam, N. Fujita, S. Shinkai, K. Kim, *Angew. Chem.* **2007**, *119*, 214; *Angew. Chem. Int. Ed.* **2007**, *46*, 210.
[15] M. J. W. Ludden, D. N. Reinhoudt, J. Huskens, *Chem. Soc. Rev.* **2006**, *35*, 1122.
[16] S. Y. Park, A. K. R. Lytton-Jean, B. Lee, S. Weigand, G. C. Schatz, C. A. Mirkin, *Nature* **2008**, *451*, 553.
[17] J. F. Stoddart, H. R. Tseng, *Proc. Natl. Acad. Sci. USA* **2002**, *99*, 4797.
[18] Y. Liu, H. Wang, P. Liang, H. Y. Zhang, *Angew. Chem.* **2004**, *116*, 2744; *Angew. Chem. Int. Ed.* **2004**, *43*, 2690.
[19] G. Sun, J. Xu, A. Hagooly, R. Rossin, Z. Li, D. A. Moore, C. J. Hawker, M. J. Welch, K. L. Wooley, *Adv. Mater.* **2007**, *19*, 3157.
[20] L. Ferreira, J. M. Karp, L. Nobre, R. Langer, *Cell Stem Cell* **2008**, *3*, 136.
[21] S. R. Bull, M. O. Guler, R. E. Bras, T. J. Meade, S. I. Stupp, *Nano Lett.* **2005**, *5*, 1.
[22] P. A. Bertin, J. M. Gibbs, C. K. F. Shen, C. S. Thaxton, W. A. Russin, C. A. Mirkin, S. T. Nguyen, *J. Am. Chem. Soc.* **2006**, *128*, 4168.

[23] A. K. Boal, F. Ilhan, J. E. DeRouchey, T. Thurn-Albrecht, T. P. Russell, V. M. Rotello, *Nature* **2000**, *404*, 746.
[24] G. Wenz, B. H. Han, A. Muller, *Chem. Rev.* **2006**, *106*, 782.
[25] J. Li, X. J. Loh, *Adv. Drug Delivery Rev.* **2008**, *60*, 1000.
[26] D. W. Bartlett, H. Su, I. J. Hildebrandt, W. A. Weber, M. E. Davis, *Proc. Natl. Acad. Sci. USA* **2007**, *104*, 15549.
[27] N. C. Bellocq, D. W. Kang, X. H. Wang, G. S. Jensen, S. H. Pun, T. Schluep, M. L. Zepeda, M. E. Davis, *Bioconjugate Chem.* **2004**, *15*, 1201.
[28] M. E. Davis, M. E. Brewster, *Nat. Rev. Drug Discovery* **2004**, *3*, 1023.
[29] According to mass spectrometry analysis, 4*-Ad-PAMAM is composed of six different Ad-substituted PAMAMs, including 2-Ad-PAMAM, 3-Ad-PAMAM, 4-Ad-PAMAM, 5-Ad-PAMAM, 6-Ad-PAMAM and 7-Ad-PAMAM. See detailled MS data in the Supporting Information.
[30] L. J. Peek, C. R. Middaugh, C. Berkland, *Adv. Drug Delivery Rev.* **2008**, *60*, 915.

